



HAL
open science

Experimental study of the effect of the long chimney of a closed tonehole on the sound of a bassoon

Augustin Ernoult, Timo Grothe

► **To cite this version:**

Augustin Ernoult, Timo Grothe. Experimental study of the effect of the long chimney of a closed tonehole on the sound of a bassoon. 2022. hal-03789436v1

HAL Id: hal-03789436

<https://hal.science/hal-03789436v1>

Preprint submitted on 27 Sep 2022 (v1), last revised 17 Feb 2023 (v3)

HAL is a multi-disciplinary open access archive for the deposit and dissemination of scientific research documents, whether they are published or not. The documents may come from teaching and research institutions in France or abroad, or from public or private research centers.

L'archive ouverte pluridisciplinaire **HAL**, est destinée au dépôt et à la diffusion de documents scientifiques de niveau recherche, publiés ou non, émanant des établissements d'enseignement et de recherche français ou étrangers, des laboratoires publics ou privés.

Experimental study of the effect of the long chimney of a closed tonehole on the sound of a bassoon

Augustin Ernout^{1, a} and Timo Grothe²

¹*Project-team Makutu, Inria Bordeaux Sud-Ouest, Université de Pau et des Pays de l'Adour, E2S UPPA, CNRS, 200 avenue de la vieille Tour, 33405 Talence Cedex, France*

²*Erich Thienhaus Institut - Hochschule für Musik Detmold, Neustadt 22 D - 32756 Detmold, Germany*

(Dated: 27 September 2022)

The bassoon has side holes a few tens of millimeters long, much longer than in other woodwinds. When they are closed, the “quarter-wave” resonances of these “chimneys” create short circuits in parallel with the bore. At these resonance frequencies, near 2 kHz –within the sensitive range of hearing– it is expected that the waves will not propagate down the chimney, affecting both the input impedance and the radiated sound. Using parametric studies with varying chimney lengths, these effects on impedance and radiated sound are measured for a French bassoon and a simplified conical model instrument. The effects are clear on the model instrument, especially when several chimneys have equal length. For the bassoon, the passive filter effect remains, but its importance on the sound is blurred due to changes in the oscillation regime and in the directivity, as simulations confirmed. The effect is audible under laboratory conditions, but in the same order of magnitude as the spatial level variations due to the directivity. Therefore, it is unlikely that under normal playing conditions a chimney length elongation of 5 mm, as found between German and French bassoon, would result in a significant change in timbre.

[<https://doi.org/DOI number>]

[XYZ]

Pages: 1–14

I. INTRODUCTION

From a mechanical point of view, a wind instrument is composed of two parts: the oscillator (reed, lips or jet) generating the acoustic vibration, and the body which has two acoustic functions. The body of the instrument delimits an air column that vibrates and, through the resonance phenomena, selects the frequency at which the instrument sounds. This role of a resonator is generally associated with the instrument’s driving point impedance, classically referred to as the acoustic input impedance (Chaigne and Kergomard, 2016, Chap.7). The second function, less studied, is sound radiation. The body influences how each frequency component of the sound is radiated into the room in terms of magnitude and directivity and so affects the frequency content of the perceived sound. Some recent studies propose to use transfer functions between acoustic quantities at the reed position and into the room to characterize this radiator function (Grothe and Amengual Gari, 2019; Petersen *et al.*, 2022).

In some wind instruments (mostly woodwinds) side holes are drilled through the wall of the body, allowing

the pitch of the sound to change. At low frequency, when a hole is open, it imposes a node of pressure at its location, which has the effect of reducing the effective length of the body of the instrument and to increase its frequency of resonance. When a hole is closed its chimney pipe can at low frequency be seen as additional volume (Chaigne and Kergomard, 2016, Chap.7.7.5.2) slightly elongating the effective length (Debut *et al.*, 2005).

However, the chimneys can also be seen as side branches of the main bore pipe. Here, the enclosed air can act as additional acoustic compliance, as described by Pierce (1989, chap.7.4, chap.7.7) for the Helmholtz resonator. At some specific frequencies, the acoustic wave is completely reflected at the side-branch. As the wave does not propagate downstream in the main duct, the branch then acts as an acoustic notch filter. This principle can be used to design a passive reactive muffler, with an array of side-branches of different lengths as proposed by Tang (2012) in air conditioning systems. For a closed cylindrical side-branch of length L , the notch occurs at a frequency corresponding to a wavelength $\lambda \approx 4L$, hence coining the term “quarter wavelength resonators” (Field and Fricke, 1998).

This effect also influences the behavior and the radiated sound of wind instruments. In most of them the

^aaugustin.ernout@inria.fr

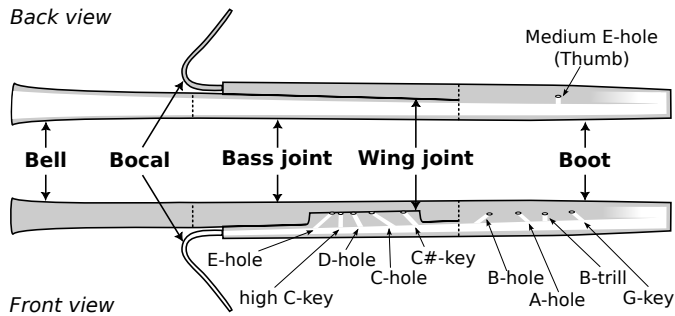


FIG. 1. Sketch of a French bassoon (back and front view). For readability, only half of the air column (in white) is plotted on each view (between the reed and the boot bend on the front view, and between the boot bend and the bell on the back view), and only the holes with the longest chimneys are represented.

chimneys are relatively short ($L < 7$ mm), giving high characteristic frequencies ($f > 10$ kHz). However, the bassoon has very long chimneys, sometimes longer than 40 mm ($f \approx 2$ kHz). This is a peculiarity of the bassoon, related to its length. To place the holes at appropriate positions in the air column, and to still be able to close them with the fingers, the corresponding holes are drilled with strong inclination (alternatively: obliquely) into a corpus part named the “wing joint” with a locally thickened wall (Fig.1). These long chimneys have been conserved during the evolution of the instrument. The possibility that they contribute to the specific sound color of the instrument may be one of the reasons for the low success of bassoons with short chimneys built during the 19th century (Kergomard and Heinrich, 1975).

Following acoustic arguments similar to the ones evoked previously, J. Kergomard suggests that these long chimney pipes, closed for the majority of the notes, induce a notch near 2 kHz in the radiated spectrum of the bassoon (Kergomard and Heinrich, 1975) (Chaigne and Kergomard, 2016, chap.7.7.5, p.374). He illustrates this by a spectrogram of a chromatic scale of a French bassoon. More recently, Petersen *et al.* (2021), in a study on a series of tone holes (called the “tone hole lattice”) of the bassoon, advance and complete this study by an up-to-date theoretical approach. The two studies suggest that this phenomenon is one explanation for the timbre difference between French and German bassoons, as for the latter the chimneys are 5 mm shorter on average (Kergomard and Heinrich, 1975; Nederveen, 1998).

However, in these two studies, the experimental data provided are purely qualitative and the notch is quite difficult to observe. Furthermore no parametric study demonstrates the relationship between the length of the long chimney and the slight notch observed in experimental data.

Indeed, in musical instruments, the acoustic source does not provide the same amount of energy at all frequencies. For a conical instrument, the spectrum of the pressure at the reed location resembles the shape of a *sinc*

function (Kergomard *et al.*, 2019). It is then difficult to distinguish if a notch in the external sound spectrum is due to a lack of energy at the reed or a muffling effect by the chimneys. Furthermore, the sound energy mainly decreases with the frequency. The range of 2 kHz, where the phenomenon occurs, corresponds in the medium register to about the 10th harmonic. Here the partials’ levels are already low (Petersen *et al.*, 2021). The alteration could be inoperative or imperceptible. Finally, due to the coupling between air-column and reed, the modification of the radiated spectrum by the long chimneys can have two origins. The first possibility relates to the resonator function: the reed motion is affected by the alteration of the input impedance; the second possibility relates to the radiator function: only the radiation efficiency of each component is altered. Of course, both functions could also simultaneously affect the spectrum.

The aim of this study is to clarify how the presence of a long chimney pipe affects the radiated sound of the bassoon. The main goal is to identify and quantify the modification of the radiated spectrum by the presence of long closed chimney pipes and to correlate this effect to their length. A secondary objective is to distinguish whether this modification is a consequence of an alteration of the reed motion or simply a passive acoustic filter effect. Finally, this study provides estimates of the perceptual importance of this phenomenon for bassoon timbre.

We propose here two experimental set-ups in which the length of the chimneys can be modified. Two instruments are played by an artificial mouth: a French bassoon and a simplified instrument with three chimneys. As it is difficult to study experimentally the behavior of the reed, simulations are carried out in parallel with these measurements. These tools allow the study of the modification of the external sound and in the pressure in the reed, when the chimneys’ length are varied, while all other parameters are kept constant.

In Section II, the instruments studied are presented. The experimental devices (the impedance sensor and the artificial mouth), and the signal processing used are then briefly described. This “material and methods” section finishes with the presentation of the models used to compute the impedance and the sound synthesis. Section III presents the effect of the long chimneys on the input impedance, the radiated spectrum and the reed pressure spectrum for the two measured instruments and the simulation. These observations are then discussed in Section IV and compared to other sources of the sound spectrum modification. Finally, the conclusions of this study are presented in Section V.

II. MATERIAL AND METHODS

A. Instruments

The bassoon studied here is a Buffet Crampon French Bassoon from 1903. Its entire geometry has been measured with split ball probes (Diatest, Darmstadt,

name	distance [mm]	height [mm]	radius [mm]	f_{chim} [kHz]
E-hole	490	45.5	2.1	1.76
high C-key	507	22.5	2.4	3.33
D-hole	572	37.0	3.0	2.10
C-hole	615	40.5	2.5	1.94
C \sharp -key	659	33.5	1.7	2.36
B-hole	830	35.5	3.6	2.14
A-hole	903	29.2	3.8	2.53
B-trill	968	28.5	2.9	2.63
G-key	1008	31.5	4.0	2.43

TABLE I. Dimensions of the French bassoon’s holes with a chimney pipe longer than 20mm: the commonly used names, the distance to the entrance, the chimney height, the internal radius and the characteristic frequency (Sec.III A).

Germany), allowing measurement of diameters with an accuracy about 0.1 mm, and a caliper. Specific attention has been given to the side hole dimension. The dimensions of the nine longest holes are visible in Table I ¹.

In this study, a focus is given to an alternative C \sharp 3 fingering of the bassoon (middle range), corresponding to a regular C3 in which the C \sharp -key is open. Here only the three finger holes with the longest chimneys (E-hole, D-hole and C-hole, see Table I) are closed. Other closed holes in this fingering are some register and sharp/flat key holes, all of which have chimney lengths shorter than 29 mm and are located after open holes. Thin-walled cylindrical tubes with a sliding piston inside were inserted into the chimneys of these three finger holes of the real bassoon. The length of these chimneys can thus be adjusted between 10 mm and 90 mm. The modifications are made keeping the original height offsets between the chimneys (E-hole: +5 mm, D-hole: -3.5 mm, C-hole: 0 mm).

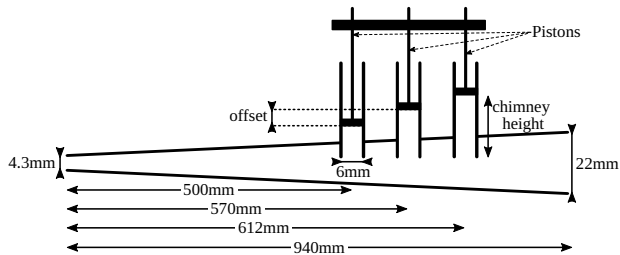


FIG. 2. Sketch of the conical instrument with 3 side holes of adjustable chimney height.

To highlight the effect of the long chimneys, a simplified bassoon is studied: a conical frustum with three side holes of adjustable chimney height (Fig. 2). The bore dimensions have been obtained by inversion with the software Openwind (Ernoul *et al.*, 2021; Openwind,

2022) by fitting the input impedance of the C \sharp 3 fingering of the French Bassoon. The conical pipe is built by coiling a gel filter sheet. It is 940 mm long and its internal radius is 2.15 mm at the entrance and 11 mm at the output, with a wall thickness of about half a millimeter. Its input impedance has been measured and compared to simulations to validate this manufacturing process (see sections II B 1 and II C 1). Standard bassoon reeds can be plugged into it. The three holes have an internal radius of 3 mm. Their chimney lengths are adjustable with a sliding piston inside the chimney pipe and can vary between 0 and 100 mm. The side holes are located at 500 mm, 570 mm and 612 mm from the entrance of the cone which correspond approximately to the locations of the finger holes in the bassoon (Tab.I).

Unlike in the bassoon in which the finger holes are drilled obliquely, in the simplified instrument, the three chimneys are parallel. This gives the possibility to hitch the three pistons together (with or without offset) and adjust the length of the three chimneys simultaneously and continuously during the experiments. Two configurations are measured: a) no offset, the 3 chimneys have the same length; b) offsets of -5 mm, 0 mm and 5 mm, giving three different chimney lengths with deviations of the same order of magnitude as for the bassoon.

B. Experimental set-up and signal processing

Mainly two experimental set-ups are used in this study: an impedance sensor and an artificial mouth.

1. Impedance sensor

The impedance sensor is an adaptation of the Two Microphone Three Calibration method (Gibiat and Laloë, 1990). It has been designed especially for instruments with small input radius (oboe or bassoon) (Eddy, 2016). The probe has an internal radius of 2 mm and is equipped by four microphones allowing the measurement of the impedance from 20 Hz to 5 kHz with good accuracy. The measured microphone signals are analyzed following the impedance calibration proposed by Dickens *et al.* (2007) to compute the input impedance.

2. Artificial mouth

The artificial mouth used is the one designed by Grothe (2013, 2015). The lip position, the lip force and the supply pressure can be adjusted. The following parameters are measured: lip force, “mouth cavity” pressure, reed internal pressure, mean flow, and the temperature. For both cone and bassoon, the same plastic reed (Premium Plastic 270M, Conn-Selmer, Elkhardt, USA) is used. The use of micrometer screws to adjust lip position and lip force achieves a very good reproducibility of experiments with the same synthetic reed (Grothe and Baumgart, 2015). The sound is recorded in a recording studio with room dimensions 5.7x5.2x3.6 m³ and 0.3 s average reverberation time using a measurement microphone (4190, Brüel&Kjær, Nærum, Denmark). The cone

with a single radiating opening is placed 1 m from this opening, in line with the main bore axis. For the bassoon, it is placed perpendicular to the main axis at 1.4 m from the D-hole in the middle of the resonator (Fig.1). As the study is focused on the variation of the sound with respect to the length of the chimney, the exact location of the microphone is not crucial as it is kept constant during all measurements. For the bassoon only the C \sharp 3 is played with different chimney length configurations. The lip force and the supply pressure are adjusted to play a C \sharp 3 “in tune” for the shortest chimney lengths. For the cone the artificial mouth parameters are adjusted to produce a stable sound at constant pitch. The fundamental frequency varies by a few percent with the modification of the chimney length given a mean value of 137 Hz for the bassoon and 130 Hz for the simple cone.

For reed instruments, the same set of parameters can lead to a different oscillation regime depending on the way these values are reached, as illustrated for the saxophone by [Colinot et al. \(2020\)](#). Due to this high sensitivity of the produced sound to the artificial mouth parameters, it is necessary to measure one given set of data without shutting down the mouth and within a relatively short amount of time. With the cone, one long recording of 30 seconds is carried out and the chimney lengths are continuously varied during the measurement. During that time, the chimney length is altered back and forth over its whole adjustment range to confirm the stability of the artificial blowing. The chimney pistons are moved together and their relative positions are acquired continuously during the experiment thanks to a draw wire position sensor (SP2, Celesco, Chatsworth, USA). For the bassoon, due to the oblique chimney angles, the chimney lengths need to be adjusted independently at the pistons using a caliper. To accomplish this, we employ a repeated capture scheme, recording one second of steady sound after each length adjustment step. The artificial mouth is not stopped in between each step. The experimenter steps back from the instrument behind a mobile absorber during the recording to avoid disturbance of the directivity pattern. As those measurements are much longer than the ones with continuous length variation, only steps of 10 mm are measured to avoid too big variation of the playing conditions.

3. Sound signal processing

To estimate the harmonic content of the external sound and the internal reed pressure, a specific signal processing for sustained tones is used: the period-synchronized sampling ([Grothe, 2013](#)). After an analysis of zero crossings, the waveform is split into successive periods. Linear interpolation is used to resample each of these periods between zero crossings to avoid leakage. The signal energy in each single period is distributed in the frequency domain across components harmonic to the respective f_0 . Redistributing these spectra on the continuous time scale leads to a spectrogram with non-equidistant time scale, time-varying frequency resolution and only harmonic components. For the cone experi-

ment with continuous length variation, the spectra are redistributed on a chimney length scale instead of a time scale. This alternative representation readily maps the influence of the chimney length on the spectrum. In the bassoon experiment with discrete chimney length variations, the same processing has been used to preserve comparability. Here, all periods of one capture were averaged in the time domain and the spectrum of this unique period, corresponding to the respective discrete chimney length, is computed.

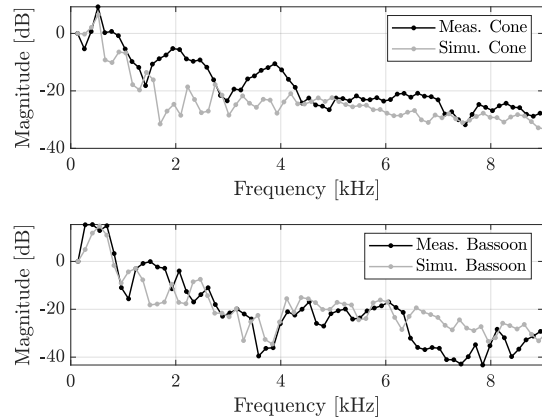


FIG. 3. Magnitude of harmonic components of the room pressure averaged for all the chimney length and scaled by the fundamental component magnitude. Top: simple conical instrument measured (black) and simulated (gray); Bottom: French bassoon measured (black) and simulated (gray).

Before looking for the quarter-wavelength-effect, an average response was obtained by averaging the magnitudes of each partial A_i over all chimney heights. These mean spectra \bar{A}_i are plotted, for both instruments, on Figure 3. As expected for conical instrument, the spectra show regular notches ([Kergomard et al., 2019](#)), most clearly visible for the simplified instrument (Fig. 3 top, at 1.5 kHz, 3 kHz, etc), but less clear for the bassoon (Fig. 3 bottom). This can be due to the complex directivity pattern of the bassoon combined with the measurement at one point. It can already be noticed that, in the frequency range around 2 kHz in which a “muffling effect” is expected (Tab.I), the radiated level is relatively low compared to the loudest partials (≈ -15 dB).

To highlight the variation of the harmonics’ magnitudes with chimney length in the rest of the study, only

$$\Delta L_i = 20 \log_{10} \left(\frac{A_i(n)}{\bar{A}_i} \right), \quad (1)$$

the deviation in decibel of the magnitude of each harmonic component A_i to its mean value over the entire measurement set \bar{A}_i is displayed. The analysis is computed period by period and the variation of the fundamental frequency and harmonics frequencies (within 1%

for each measurement) is not represented. For readability reasons, in the rest of the study and in the graphs, each partial is named by its average frequency in kHz.

C. Numerical simulation

All simulations are made with the software [Openwind](#) (2022). This includes simulations of the acoustical behavior of the air column (Section II C 1), the reed-resonator interaction (Section II C 2), and the radiated sound (Section II C 3).

1. Input impedance

The body of the instrument is modeled as a network of pipes (main bore and side holes). For a pipe of length ℓ , the acoustic pressure $P(x, \omega)$ and flow $U(x, \omega)$ are computed with the telegrapher's equation, written here in the frequency domain:

$$\begin{cases} \ell Z_v(x, \omega) U_n + \frac{dP}{dx} = 0 \\ \ell Y_t(x, \omega) P_n + \frac{dU}{dx} = 0 \end{cases} \quad \forall x \in [0, 1], \quad (2)$$

where Z_v and Y_t are the viscous impedance and thermal admittance modeling the losses (Zwikker and Kosten, 1949) (Chaigne and Kergomard, 2016, chap.5.5). At the junction between the main bore pipe and a chimney, the relation between the volume flow u_1, u_2, u_3 and the pressure p_1, p_2, p_3 at each pipe end (upstream part, downstream part and chimney) is given by the equation (Ernoul et al., 2021)

$$j\omega \begin{pmatrix} m_{11} & m_{12} \\ m_{12} & m_{22} \end{pmatrix} \begin{pmatrix} u_1 \\ -u_2 \end{pmatrix} = \begin{pmatrix} 1 & 0 & -1 \\ 0 & 1 & -1 \end{pmatrix} \begin{pmatrix} p_1 \\ p_2 \\ p_3 \end{pmatrix} \quad (3)$$

$$u_1 - u_2 - u_3 = 0.$$

where m_{ij} are acoustic masses (often expressed in equivalent lengths) related to geometry of the junction (Lefebvre and Scavone, 2012).

The boot bend of the bassoon is modeled as a straight cone, the length of which is tuned to conserve the volume of the actual geometry.

To compute the impedance, Equations (2) are solved in the frequency domain using 1D finite elements for the spatial discretization. A unitary flow is imposed at the entrance for each frequency. In this case, the radiation impedances are computed with the non-causal fit proposed by Silva et al. (2009). More technical details on the impedance computation can be found in previous articles (Ernoul et al., 2021; Tournemenne and Chabassier, 2019).

2. Reed-Resonator Interaction

To synthesize the sound of the two instruments it is necessary to solve the telegrapher's equation Eq. (2) in the time domain. In addition to the FEM, an energy-based method is used to discretize the wave equation

in time, using a diffusive representation to model the thermo-viscous losses. The scheme used and its implementation are detailed by Thibault and Chabassier (2021). For the radiation conditions, a first order Padé development is used, following for example the work of Rabiner and Schafer (1978).

A tube modeling the wave propagation inside the reed must be added at the entrance of the instrument. The effective geometry of this tube is set to a cylindrical tube having the same internal diameter as the output of the actual reed: 5.3 mm. Its length is chosen so that its acoustic characteristics correspond to those of the real reed. To do this, the impedance of the reed is measured at its output. The length is then tuned by fitting the simulation to the measurement with the optimization tool of the Openwind software (Ernoul et al., 2021). The length obtained is 45 mm, giving a reed volume about 1 cm³.

The equations used to model the double reed are strongly inspired from the work of Bilbao (2009). The numerical schemes used have been refined by Thibault and Chabassier (2020), to be energy preserving (Openwind, 2022). The double reed is described as an oscillator with one degree of freedom, characterized by a set of effective coefficients: the equilibrium height of the reed's channel H_r , the width of the channel W_r , the effective stiffness K_r , the effective oscillating surface of the reed S_r , the natural frequency ω_r and the quality factor Q_r . This set of coefficients is completed by the supply pressure p_m . The distance between the reed blades $y(t)$ is given by this system of equations:

$$\begin{aligned} \ddot{y} + \frac{\omega_r}{Q_r} \dot{y} + \omega_r^2 (y - H_r) &= -\frac{\omega_r^2}{K_r} \Delta p \\ \Delta p &= p_m - p_{in} \\ u_m &= W_r [y]^+ \sqrt{\frac{2|\Delta p|}{\rho}} \text{sign}(\Delta p) \\ u_{in} &= u_m - S_r \dot{y} \end{aligned} \quad (4)$$

where u_{in} , p_{in} the acoustic flow and pressure at the entrance of the instrument and where $[y]^+$ refers to positive y (when the reed is open). Since the goal of the simulations is not to reproduce the exact waveform but to observe how the sound is affected by the long chimney, the model is simplified by neglecting the contact force between the reed blades. They can interpenetrate ($y < 0$), in which case the flow is zero. As discussed by Colinot et al. (2019), this "ghost reed" simplification influences the sound spectrum but not the behavior of the instrument.

The height H_r , is estimated from a close-up frontal image of the reed inlet. To measure the natural frequency of the reed ω_r and the quality factor Q_r , the reed is plugged on a cylindrical tube in which a loud speaker injects an acoustic chirp. A laser vibrometer (PDV100, Polytec, Waldbronn, Germany) measures the pressure-induced vibration of the tip of the reed. The frequency at which the response is maximal gives the natural frequency ω_r , and the -3 dB bandwidth, the quality factor. Their values hardly seem to depend on the lip force. The equilibrium height H_r , the natural frequency ω_r and the quality factor Q_r can be measured in the same configura-

p_m	measured	3.58 kPa
u_A	measured	0.79 L/s
p_M	measured	8.76 kPa
H_r	measured	1 mm
ω_r	measured	$2\pi \times 1700$ rad/s
Q_r	measured	14.5
W_r	$\frac{u_A}{H_r \sqrt{2p_M/\rho}}$	6.5 mm
K_r	p_M/H_r	8.76 kPa/mm
S_r	tuned	0.75 ; 1.05 cm ²

TABLE II. Values of reed parameters used for sound synthesis. Only the section S_r has a different value for the bassoon ($S_r = 0.75$ cm²) and for the conical instrument ($S_r = 1.05$ cm²).

tion used to play the instruments due to the transparency of the walls of the artificial (Grothe, 2013).

The measurement of the quasistatic pressure-flow characteristic allows the indirect estimation of the effective width of the reed channel W_r and the effective mass M_r . Due to the small diameter of the reed (about 5 mm), the classical methods to avoid reed oscillations cannot be used (diaphragm (Dalmont *et al.*, 2003) or anechoic cylindrical tube which imposes too strong flow resistance). Instead, some foam is added as flow resistance in the upper joint of the bassoon and a mass of clay is stuck on the reed blades which does not affect the quasistatic behavior. The pressure p_m is then increased step by step. In quasistatic conditions, Eq. 4 becomes the valve-characteristics of the reed

$$u_m = u_A \left(1 - \frac{\Delta p}{p_M} \right) \sqrt{\frac{\Delta p}{p_M}}, \quad (5)$$

with $p_M = K_r H_r$, the closing pressure and $u_A = W_r H_r \sqrt{2p_M/\rho}$, a characteristic flow. By fitting this classical model to experimental data, parameters u_A and p_M have been determined to represent the embouchure in the artificial blowing experiment (Tab.II). The obtained values are consistent with previous measurements (Grothe, 2015).

The effective surface S_r cannot be easily measured. Its value is tuned by trial and error to obtain about the same fundamental frequency in simulation and measurements given two different values for the bassoon and the simple conical instrument (on average, respectively a 6 cent and 18 cent difference in pitch).

The sound simulations are run for different chimney lengths in 1 mm steps for the simple instrument and 5 mm steps for the bassoon. For each configuration a sound simulation of 0.5 s is computed. The mouth pressure increases linearly from 0 Pa to the target supply pressure p_m in 20 ms. The transients are excluded by analyzing only the last 100 ms of each simulation. To study the properties of the source, the position of the reed as well as the flow rate and the acoustic pressure at

the input of the air column are recorded. Their spectrum is processed in a similar way to the bassoon experimental signal (Sec.IIB3) to obtain the variation of the partials with respect to the length of the chimneys.

3. Radiation

The radiation is studied through the total power radiated at each frequency $P_{rad}(\omega)$. It corresponds to the integration of the acoustic intensity over a sphere surrounding the instrument. This quantity excludes the effects of directivity and can be seen as the mean sound spectrum. For the bassoon radiating from multiple source locations (open holes and bell), it is computed as the sum of the power radiated by each opening at each frequency:

$$P_{rad}(\omega) = \sum_{n=1}^N P_{rad}^{(n)}(\omega) \quad (6)$$

The power $P_{rad}^{(n)}(\omega)$ radiated at the n^{th} opening is computed from the spectrum of the flow $|U_n(\omega)|$ at this opening in playing conditions as (Chaigne and Kergomard, 2016, chap.12.3.3, p.642):

$$P_{rad}^{(n)}(\omega) = \frac{1}{2} \Re(Z_{rad}) |U_n(\omega)|^2 \approx \frac{\rho}{8\pi c} \omega^2 |U_n(\omega)|^2. \quad (7)$$

where $U_n(\omega)$ is the magnitude of the volume velocity at the frequency ω . This is computed from the simulated temporal signal with the same signal processing as the experimental data (Sec.IIB3).

The simulations' spectrum, averaged over all chimney lengths, is compared to that of the measurements in Figure 3. Since the "ghost reed" approximation tends to underestimate the magnitude of the high frequency components, the observed discrepancy between the simulated and measured data is expected. This lack of high frequencies is more pronounced for the simple instrument (Fig. 3, top). For the bassoon (Fig. 3, bottom), an acceptable general agreement is found in the range [2, 6] kHz. In addition, the formants around 0.5 kHz, and the notches around 1 kHz and 3.5 kHz are approximately predicted. Beyond neglecting the contact force, the deviation at low (< 1 kHz) and high frequencies (> 6 kHz) can also be a consequence of the use of a single microphone for experimental data combined with the spatial distribution of the acoustic fields (e.g., directivity of the instrument, room reflections, etc). In simulations, all these effects are not treated due to the observation of the total radiated power.

However, since the analysis is focused on the relative variation in harmonic content due to the change in chimney length, these discrepancies between simulations and measurements are not critical here: the goal is simply to validate whether the simulations are able to predict how long chimneys affect the radiated sound and not whether they correctly predict the sound, in absolute terms.

III. RESULTS

A. Effect on the impedance

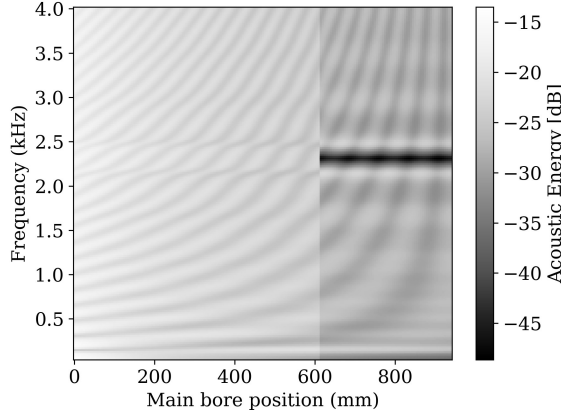


FIG. 4. Simulation of the acoustic energy distribution along the main bore of the simplified instrument with the third chimney pipe set to 35mm and the two other to 0. The energy is scaled by the mean energy in the instrument for each frequency.

As already discussed by Petersen *et al.* (2021), the presence of long chimneys affects the wave propagation along the main bore of the instrument at specific frequencies. The chimney pipe acts as a muffler which “traps” acoustic energy at its characteristic frequency, and dissipates it through visco-thermal effects. To illustrate how this affects the input impedance of the instrument, the wave propagation into the simplified cone with only one closed chimney (located at 612 mm with a length of 35 mm, see Fig. 2) is simulated.

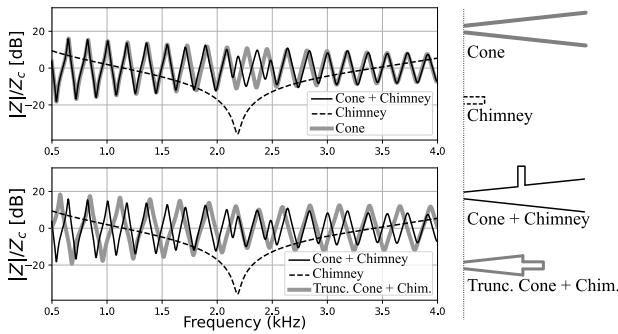


FIG. 5. Input impedance of the simplified instrument with one closed long chimney (thin black line) and of the closed chimney alone (thin dashed line). Top: input impedance of the cone without side hole (thick grey line). Bottom: input impedance of the cone truncated at the hole location and extended by the closed chimney (thick grey line).

The acoustic energy distribution along the main bore for each frequency is represented on Fig. 4. The energy $E(f, x)$ at the frequency f and the location x is defined as:

$$E(f, x) = \frac{1}{2} \Re(Y_t(f, x)) |p(f, x)|^2 + \frac{1}{2} \Re(Z_v(f, x)) |u(f, x)|^2 \quad (8)$$

Figure 4 representing only the energy along the main bore, the darker color shading downstream of the hole location at 612 mm distance from the entrance illustrates that some of the energy is in the hole chimney. For a very specific, narrow frequency band (here around 2.3 kHz), there is no more energy in the main pipe beyond the closed side hole (position > 612 mm). This phenomenon, already observed by Petersen *et al.* (2021) has a direct influence on the acoustic impedance at the driving point (input impedance).

At the junction point between the main bore and the side hole, the chimney pipe and the downstream part of the cone can be seen as two pipes in parallel, each with their own impedance $Z_{chim}(f)$ and $Z_{down}(f)$. The effective impedance is

$$Z_{eff} = \frac{1}{\frac{1}{Z_{chim}} + \frac{1}{Z_{down}}} \quad (9)$$

As mentioned by Chaigne and Kergomard (2016, chap.7.7.5), it is important to include in Z_{chim} the masses of the junction (Eq. 3). At the characteristic frequency of the chimney ($f = f_{chim}$) the chimney impedance at the bore junction is very low (a pressure node), we have $Z_{chim}(f_{chim}) \ll Z_{down}(f_{chim})$. The chimney pipe can then be seen as a short circuit and $Z_{eff}(f_{chim}) \approx Z_{chim}(f_{chim})$. This can be directly observed in the input impedance (Fig. 5).

The open cone with closed chimney (see curve “Cone+Chimney”, Fig. 5) behaves like an open cone without a chimney (see curve “Cone”, Fig. 5, top) for most of the frequency range. Only near the characteristic chimney frequency, around 2.3 kHz (see curve “Chimney”, Fig. 5), does it behave like a shortened cone, truncated and closed at the hole junction and extended by the closed chimney (see curve “Trunc. Cone + Chim”, Fig. 5, bottom). The frequency range at which this phenomenon occurs is therefore only related to the length of the chimney pipe. But the value of the input impedance of the total instrument in this range depends also on the location of the hole. The modification of the effective length of the instrument due to this phenomenon can also be observed in Figure 4. The regular evolution of the energy distribution along the main bore with respect to the frequency is disturbed in the range 2 - 2.5 kHz.

It is interesting to notice that this local modification of the impedance occurs both for open or closed holes. However, for a closed hole, the characteristic frequency is about half that of an open hole with the same dimensions (closed: $f_{chim} = (2n + 1)c/(4\ell)$; open: $f_{chim} = (n + 1)c/(2\ell)$, with $n \in \mathbb{N}_0$, c the speed of sound and ℓ the chimney length). At the same characteristic

frequency, an open hole of twice the chimney length produces a similar disturbance of the input impedance. However, the effect on radiated sound is very different. Both the closed hole and the open hole (of double length) attenuate the propagation downstream in the main duct. But, the frequency component is still radiated by the open hole while it is not by the closed hole.

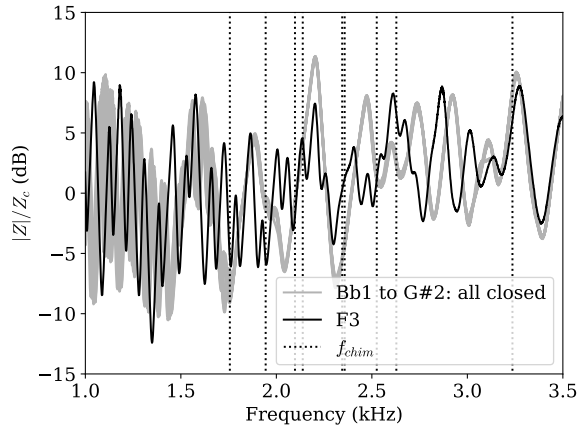


FIG. 6. Comparison of the input impedances of a French bassoon for several fingerings. Grey lines: superposition of the input impedance of the 10 lowest fingerings (Bb1 to G#2) for which all the holes with chimney longer than 20 mm are closed. The F3 fingering for which the five longest chimneys are open (black line) has a different pattern. Vertical dashed lines: characteristic frequencies of longest chimneys (Tab.I).

This phenomenon occurs in all wind instruments with side holes. It has raised little interest so far, possibly because for most wind instruments except the bassoon the chimney lengths are small ($\ell < 7$ mm) such that the muffler effect of the closed holes occurs at frequencies $f_{chim} > 10$ kHz higher above the frequency range typically considered useful in impedance measurements (≈ 5 kHz (Le Roux *et al.*, 2008)). However, for the bassoon's particularly long chimneys (Tab.I), this phenomenon occurs at relatively low frequency (≈ 2 kHz) and its effects are clearly visible in impedance measurement.

In Figure 6, the impedances measured on the French bassoon for the lowest fingerings are compared. As Petersen *et al.* (2021) had already noticed, above about 1.7 kHz, the input impedances of the ten fingerings from Bb1 to G#2 are equal within the measurement accuracy (deviation < 1 dB). For these ten fingerings, all holes with chimneys larger than 20 mm are closed, as well as all other side holes located upstream of the last of these long holes. Therefore, in the frequency range where the muffling effect of a specific chimney occurs, the impedance of the ten finger-holes is similar to the impedance of the upstream portion of the instrument, truncated at the location of the hole under consideration, and extended by the closed chimney (as for the simplified instrument in

Fig.5). Although the effect of each long chimney is local along the frequency axis, the distribution of chimney lengths gives an overall effect, such that these 10 fingerings have the same input impedance throughout the observed range above 1.7 kHz.

For the F3 fingering, the five holes with the longest chimneys are open, including the ones placed the closest to the reed end (Tab.I). The impedance of this fingering diverges from the others in the entire range. Indeed, even at 2.36 kHz corresponding to the quarter-wave resonance of the longest closed hole for this fingering, the impedance diverges due to the difference in the upper part of the instrument.

B. Effect on the radiating sound

The evolution of the harmonic content of the sound pressure in the room with respect to the chimney length is plotted on Figure 7 for both the conical instrument with side holes and the French bassoon. It shows both experimental data acquired with the artificial mouth with steady control parameters, and simulations, which are computed with the same, constant parameters values (cf. Tab. II). To highlight the effect of the chimneys, the graph represents the deviation from the average magnitude of each component, i.e. the magnitude averaged over all chimney length configurations (see Eq. 1, Sec.II B 3).

Firstly, we discuss the simplified instrument, when the three chimneys have the same length (Fig.7 a and b). Notches are clearly visible in the radiated sound spectra at the frequencies of the impedance minima of the chimneys (f_{chim} , $3f_{chim}$, $5f_{chim}$, ...) both in measurement and simulation. To demonstrate this effect animated spectrograms with experimental sound data are provided as supplementary materials^{2 3}. Due to the cumulative effect of the three chimneys, when f_{chim} perfectly matches the frequency of one partial, its attenuation in the room can reach -30 dB and even -40 dB in simulated data. It is for example visible in Figure 8 (top) which shows the evolution of the amplitude of a single partial with respect to the chimney height. The partial tracked here is the one nearest 1.8 kHz, which corresponds to the characteristic frequency of the longest chimney of the bassoon (Tab. I). It is strongly attenuated when the length of the chimneys equal 45 mm. However, if f_{chim} is in between two partials the radiated sound is almost not altered, as for a chimney length of about 75 mm in Fig.7 a.

When length offsets are applied to the chimneys, a series of three notches can be observed (Fig. 7 c and d), corresponding to the characteristic frequencies of each of the chimneys. The attenuation is less pronounced (about -10 dB to -15 dB), especially for smaller chimney lengths ($\ell < 40$ mm), when their effect does not overlap in the frequency domain. However, when the characteristic frequencies are sufficiently close, a wider frequency range is affected. A complementary effect can be observed even more clearly from Figure 8 (top). This time, if an offset is applied, the considered partial near 1.8 kHz is affected by

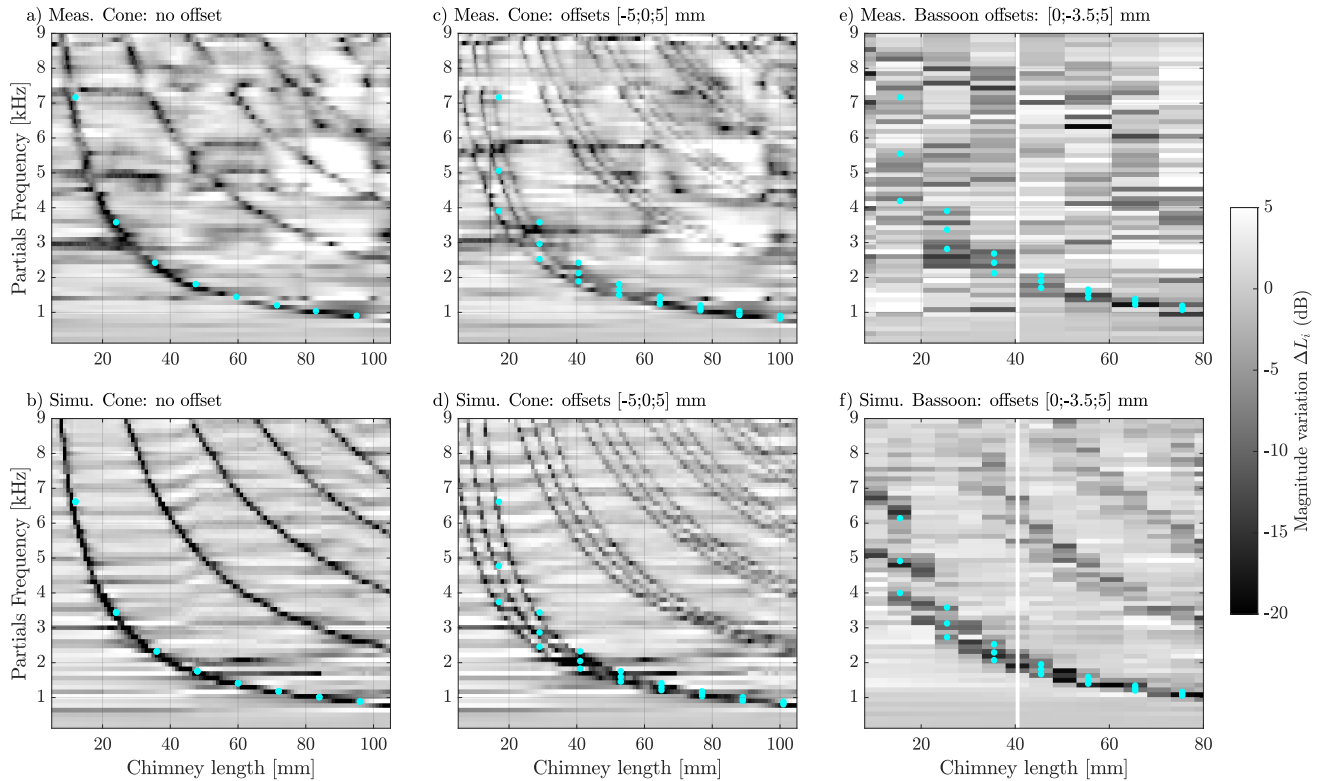


FIG. 7. Variation of the sound spectrum of note $C\sharp_3$ (Cone: $f_0 \approx 130$ Hz; Bassoon: $f_0 \approx 137$ Hz), with respect to the closed chimney length. The shading represents the level in dB with respect to the mean level per partial (cropped to [-20 dB, 5 dB] for readability). The cyan dots correspond to the characteristic frequency f_{chim} of the closed chimneys. First line (a, c, e) corresponds to measurements and second line (b, d, f) to simulations. (a) and (b): Cone with three closed chimneys of equal length; (c) and (d): Cone with three chimneys of different lengths; offset [-5mm, 0mm, 5mm]; (e) and (f): French bassoon fingered $C\sharp$, length of three original finger holes varied using a piston by keeping the original offset [0mm, -3.5mm, 5mm] (Tab.I). The white vertical line in (c) and (f) indicates the regular lengths of the bassoon’s chimneys (Tab.I)

a wider range of chimney length but with a lower amplitude. The simulations predict correctly the magnitude of the attenuation even if the affected range is slightly smaller. It can be due to a small geometric difference between the simulated and real instruments.

The simplified conical instrument discussed above is an academic example. In the following it is shown that these “notch-effects” are also present in the external sound of the bassoon, both in experiment (Fig. 7 e) and simulation (Fig. 7 f). At low frequency ($f < 3$ kHz), the magnitude of the notches in both simulations and measurements are similar, around -15 dB. This is the same order of magnitude that is observed for the simplified instrument with chimney offsets (Fig. 7 c).

The notch in the simulated data is slightly more pronounced but the general agreement is satisfying, considering the differences between measurement and simulation in terms of sound generation regimes (continuous length variation vs. step by step length variation), eventual geometric discrepancy, and in the radiated pressure field (single point vs. spatial integration) (Sec.II C 2).

At high frequency ($f > 3$ kHz), it is still possible to guess the notches in the simulated data, but not in the measurements: huge variations of the magnitude of these components appear, with no clear relation to the length of the chimneys, and disturb the observation of the quarter wavelength effect (Fig. 7 c). A possible explanation for this is a modification of the directivity pattern of the instrument due to the variation of the chimney length.

The effect of directivity can be estimated from simulations, by comparing Figure 7 d, to Figure 9 which represents the variation of the simulated power spectrum radiated by one single hole, namely the D-key hole near the boot of the instrument. The radiated power at some partials above 3 kHz strongly varies without clear correlation with the chimney length. These variations are not visible in the total radiated spectrum, suggesting that only the energy distribution between the openings is changed. As a consequence, the directivity of the instrument is also changed. It is important to note that, for the bassoon, depending on frequency, this scattering effect is stronger than the quarter wavelength effect and blurs it in exper-

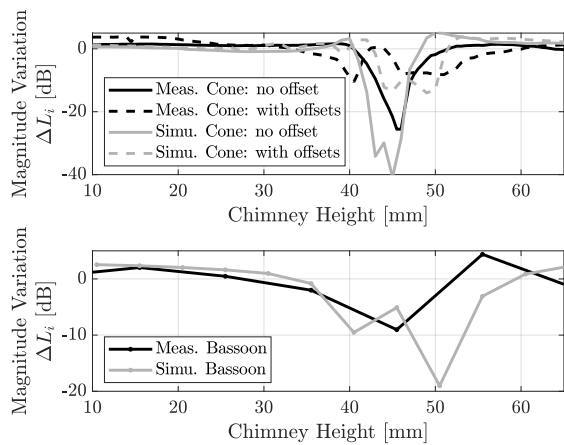


FIG. 8. Magnitude of the partial near 1.8 kHz in the external pressure spectrum of the note C \sharp 3 (Cone: $f_0 \approx 130$ Hz; Bassoon: $f_0 \approx 137$ Hz) as a function of chimney length. The magnitude is given in dB relative to the mean, and the chimney length is the instantaneous median of the three different chimneys lengths varied simultaneously. Top: simple conical instrument measured (black) and simulated (gray), without (plain line) and with offsets (dashed line) between the chimneys lengths; Bottom: French bassoon measured (black) and simulated (gray), with offsets between chimneys lengths.

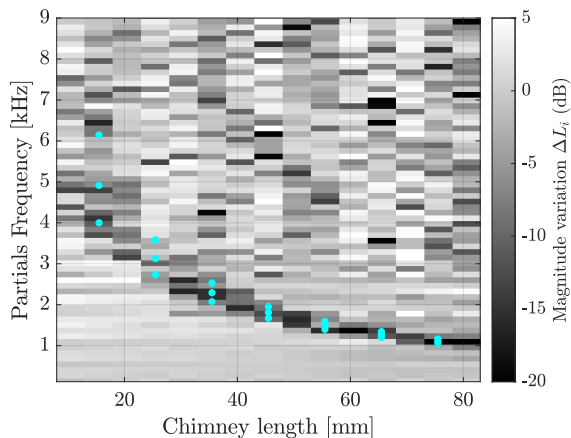


FIG. 9. Simulation of the power radiated by the D-key hole (near the boot) with respect to the chimney length. Each component is scaled by its mean magnitude.

perimental data. The simplified conical instrument having only one opening, this modification of the pattern does not happen.

In addition to the muffler effect, other changes in the radiated sound spectrum are visible in Fig.7, especially for the simple instrument. For example, the partial near 3 kHz is about 15 dB lower for chimneys shorter than 30 mm than for long chimneys. This effect is present with and without chimney length offset and in both simulated

and measured data (Fig.7.a, b, c, d). Conversely, the partial near 3.3 kHz is about 5 dB louder for the short chimneys, and so on alternately for the other partials. This effect is almost absent for the bassoon (Fig.7.e, f). These variations of the radiated spectrum can be related to the reed pressure.

C. Effect on the reed pressure

In this study, the considered quarter-wave resonances occur at frequencies much higher than the fundamental frequency of the sound ($f_{chim} > 1$ kHz, corresponding at least to the 7th partial). Moreover, the reed can be seen as a second order low-pass filter whose cut-off frequency is equal to $\omega_r/2\pi = 1.7$ kHz (cf. Eq.(4)). One could therefore assume that the quarter-wave resonances do not affect the coupling between the reed and the air column and have only a passive effect. To discuss this hypothesis, the spectrum of the pressure measured inside the double reed (reed pressure) and the spectrum of the simulated reed quantities (pressure, flow rate and position) are studied.

The variation of the spectrum of the reed pressure with respect to the chimney lengths is represented on Figure 10 for both instruments and both simulated and experimental data^{3 4}. For the simple conical instrument (Fig. 10 a, b, c, d), variations of about ± 5 dB can be observed both in simulated and measured data. As for the external sound (last paragraph of Sec. III B), the partial near 3 kHz is about 10 dB weaker for short chimneys and conversely, the partial near 3.3 kHz is about 5 dB stronger for short chimneys.

Figure 11 details the relative variation of the partial near 3 kHz of several simulated quantities for the simple instrument with chimney length offsets [-5, 0, 5] mm. The 10 dB increase in reed pressure is clearly visible. This occurs when this partial crosses the quarter-wave resonances of the chimneys (between 20 mm and 30 mm, Fig.11, top). In addition, the input impedance is slightly higher for short chimneys (Fig.11, top). These two variations together result in a 10 dB variation in input power: $\mathcal{P}_{in} \propto |P_{reed}|^2/\Re(Z)$ (Fig.11, bottom). The analysis of this partial illustrates a more global redistribution of the input power along the frequency axis. Moreover, even if this partial is higher than the cutoff frequency of the reed (Tab.II), the movement of the reed follows the variation of the reed pressure. These observations suggest that the variation in reed pressure, observed in Fig.10, is not a passive consequence of the change in impedance but results from a change in coupling between the reed and the air column. This effect is visible on the radiated power (Fig.11, bottom) which follows the evolution of the input power with frequency except when the muffling effect occurs. In this specific configuration and for this partial, the two phenomena (change in input power and muffling effect) have similar magnitudes.

For the bassoon, this effect is less pronounced (Fig. 10.e, f). This may be a consequence of the presence

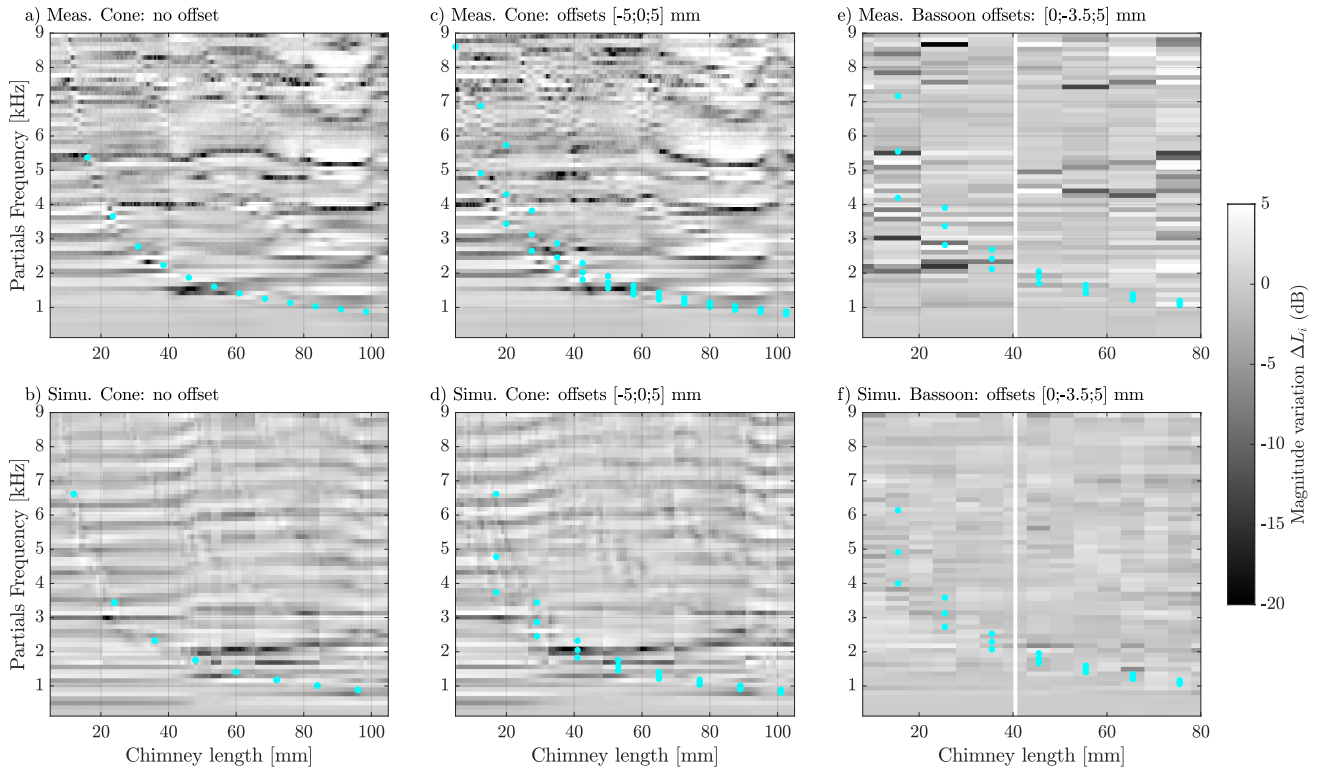


FIG. 10. Variation of the reed pressure spectrum of a played note $C\sharp_3$, with respect to the closed chimney length. See caption to Fig. 7

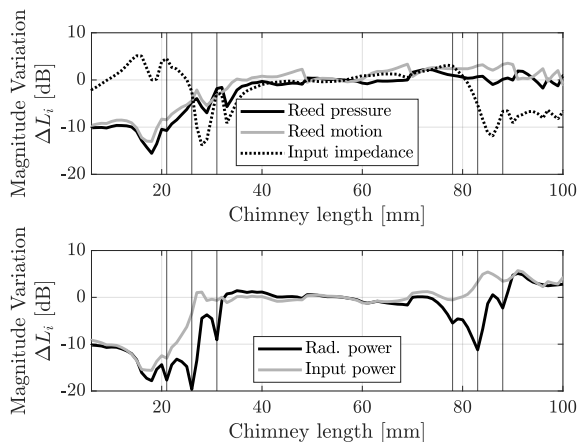


FIG. 11. Relative variation with respect to the chimney length of the spectra at the partial near 3 kHz of different simulated quantities for the cone with offsets $[-5, 0, 5]$ mm: (top) the reed pressure, the reed motion, and the input impedance; (bottom) the input and the radiated power. The vertical lines indicate the lengths for which the quarter wavelength resonance of one chimney equals 3 kHz.

of the open toneholes lattice which breaks the regularity

of the impedance peaks for frequencies above about 500 Hz (Petersen *et al.*, 2021).

However, in the bassoon experimental data (Fig. 10.e), strong fluctuations appear (± 10 dB), apparently randomly, for frequencies above 3 kHz. Absent from the simulation data, they appear to be the result of experimental problems. They could be the consequence of small fluctuations in the parameters of the artificial mouth. Indeed, as illustrated by Kergomard *et al.* (2016), the oscillation regime is very sensitive to these parameters, especially for those high partials having a relatively low magnitude compared to the lower partials (Fig.3). These fluctuations can be related to the ones observed in the external sound (Sec.III B).

IV. DISCUSSION

In this study, the experimental setup (a simplified instrument with variable chimney lengths) and the signal processing (normalization by the average spectrum) were designed to highlight the effect of long chimneys on the radiated sound. The effect is most clearly observed in the linear acoustic behavior of the air column, as a notch filter effect. It has consequences for the reed oscillation regime and also for the radiation. These three aspects, apparently large under laboratory conditions, will be set

in perspective with variations typically found in playing conditions and with their importance to the perceived sound.

Firstly, single harmonics were found to be decreased by about 10 dB. In real musical instruments, the affected harmonics were in a much higher frequency range than the fundamental pitch. For the low register of the studied French bassoon, the lowest characteristic frequency is about 1.76 kHz (Tab.I) corresponding to the 10th partial of the note E3, and the 15th partial of the note Bb1. Moreover, the radiated power of these partials is low compared to the loudest partials (-10 dB, Fig.3). The audibility of such a phenomenon is therefore not self-evident.

Secondly, it is difficult to observe experimentally the long chimney effect on a real musical instrument (Section II B 2). Already a small fluctuation of the embouchure can strongly affect the spectrum at the considered frequency and making it difficult to observe the phenomenon. Even with carefully designed artificial mouth experiments, the effect is not really pronounced (Fig. 7.c) and it is almost invisible on the absolute spectrogram not scaled by the mean magnitude of each component³.

A third aspect is the importance of the directivity at these frequencies. The results in Section III B must be seen with the regard to the variations in the instruments directivity For a German bassoon fingered for the note F3 it is larger than 25 dB (Grothe and Kob, 2019, 2020). Thus, the level difference between two locations in a room for a fixed chimney configuration can be larger than the level difference between two different chimney configurations at the same location.

To estimate the importance of single harmonics in the lower mid-frequency range on the overall sound perception, a preliminary study has been carried out. A bassoon tone has been re-synthesized from the Fourier decomposition of the measured bassoon sound. The level of the partial 15 and 16 (≈ 2 kHz) was reduced by 20 dB, presented vs. the original and asked whether the test person's could hear the difference. The perceptive threshold was searched in a 2 up 1 down scheme, adjusting the levels of the two partials according to the correctness of the test persons response. From a group of 22 Tonmeister⁵ and music students, 10 test persons showed a converging threshold near -2.5 dB (median, range -1.5 to -6 dB), the other 12 did not show any convergence.

Therefore we can assume that the decrease of 10 dB observed experimentally in a very narrow band is an effect that is identifiable in direct comparison. However, from a more global point of view, taking the variations due to the reed excitation and the radiation directivity into account, we regard the long closed chimney effect to be rather subtle for the bassoon timbre.

V. CONCLUSION

The presence of a long closed side hole affects the radiated sound of wind instruments. When the hole is closed, it induces a notch in the spectrum at a characteristic frequency corresponding to quarter wavelength

of the chimney pipe ($\lambda \approx 4L$, with L the length of the chimney). More precisely, it can attenuate the radiated power of a partial by about 15 dB if the closed chimney frequency coincides with it. The effect is even larger, when the air-column has several side holes with the same chimney length (Fig. 8).

This can be explained by the fact that, at this frequency, the input impedance of the side branch is low. Most of the acoustic energy is deviated to the closed chimney and does not propagate into the downstream part of the instrument (Fig. 4). A consequence of this effect is also seen in the air-column's input impedance which, near this frequency, approximately equals that of an instrument rigidly terminated at the location of the side branch (Fig. 5). This affects the source mechanism and induces variation up to 10 dB of the magnitude of partials in the reed pressure spectrum (Fig. 10). This effect can be also observed in the external sound (Fig. 7).

The notch filter has a quite narrow stop band. In our experiment on a cone at $f_0 \approx 130$ Hz the radiated sound was hardly affected if the characteristic frequency of the chimney was in between two partials. However, in a real instrument, the chimneys have different lengths and consequently a large frequency band can be affected by this phenomenon. This can readily be seen from the input impedance of the different bassoon fingerings which are all equal over the entire range above 1.7 kHz (Fig. 6), or for configurations with chimney length offset (Fig.8).

However, whether this effect on the global timbre of a real instrument would be noticed is still not decided. The level of harmonic components in the range where the chimney effect occurs, is very sensitive to both the reed excitation and the location of the listener. The sound spectrum of a woodwind instrument with many tone holes can be more different for two locations in a room than between two instruments having slightly different chimney lengths. In particular, comparing French and German bassoon designs, the longest chimney is only 5 mm longer in the former (Nederveen, 1998). With regard to the low frequency end of the closed chimney stop band this corresponds to a shift of 300 Hz from 1.8 kHz for the French to 2.1 kHz for the German bassoon, as an effect of one single tone hole chimney. Although an overtone level shift of a few dB in this frequency range is perceptible for trained listeners in an artificial side-by-side comparison, even a -20 dB attenuation in a narrow band with two partials seems not to change the overall timbre impression. It should be interesting to confirm this, from the players' perspective, in a specific study.

In conclusion, while the effect of a long closed chimney on the external sound can be measured and perceived under controlled conditions, it is not a predominant effect compared to other sources of spectrum variation (e.g., directivity). This effect may contribute to the specific sound of the bassoon, but it seems unlikely to hear, under normal playing conditions, the difference in timbre caused by the difference in chimney length between the French and German bassoon. The notch

near 2 kHz observed in the spectrum in previous studies (Petersen *et al.*, 2021) (Chaigne and Kergomard, 2016, chap.7.7.5.2) is probably more a consequence of the pressure spectrum of the reed having "natural" notches for conical instruments, than the quarter-wave effect of the chimney.

This study also shows that a simplified model of sound generation and radiation⁶ is able to predict the relative change in the external sound spectrum induced by a change in geometry (Fig.8), even if the absolute value of this spectrum deviates from measurements (Fig.3). Whole instrument models are not often presented in the literature and it can be emphasized that this is a further step towards computer-aided design of wind instruments.

ACKNOWLEDGMENTS

This research was supported by travel grants kindly offered by DAAD and Hochschule für Musik Detmold. We thank Zara Ali, David Gayler, Thomas Grosse, Malte Kob, Malte Schäfer and Nils Wallbaum. Stefan Pantzler provided the French bassoon, split-ball probes were provided by Diatest.

¹The term "hole" refers to holes which are closed by the fingers, holes named "key" or "trill" are closed by pads. The "E-hole" is the one opened to go from D to E.

²See Supplementary materials at [URL will be inserted by AIP]. It allow listening to the modification of the external sound as function of the chimney length for both simple instrument and bassoon.

³ The supplementary materials are also available on the companion page: https://people.bordeaux.inria.fr/augustin.ernoult/long_chimneys

⁴See Supplementary materials at [URL will be inserted by AIP]. It allow listening to the modification of the reed pressure of both simple instrument and bassoon, as function of the chimney length.

⁵musically trained sound engineers

⁶The software *Openwind* (2022) is free and open access under GPL v3 license, available at <https://openwind.inria.fr>

Bilbao, S. (2009). "Direct Simulation of Reed Wind Instruments," *Computer Music Journal* **33**(4), 43–55, direct.mit.edu/comj/article/33/4/43-55/94265, doi: 10.1162/comj.2009.33.4.43.

Chaigne, A., and Kergomard, J. (2016). *Modern Acoustics and Signal Processing Acoustics of Musical Instruments* (Springer, New York), link.springer.com/10.1007/978-1-4939-3679-3.

Colinot, T., Guillemain, P., Vergez, C., Doc, J.-B., and Sanchez, P. (2020). "Multiple two-step oscillation regimes produced by the alto saxophone," *The Journal of the Acoustical Society of America* **147**(4), 2406–2413, asa.scitation.org/doi/10.1121/10.0001109, doi: 10.1121/10.0001109.

Colinot, T., Guillot, L., Vergez, C., Guillemain, P., Doc, J.-B., and Cochelin, B. (2019). "Influence of the "Ghost Reed" Simplification on the Bifurcation Diagram of a Saxophone Model," *Acta Acustica united with Acustica* **105**(6), 1291–1294, www.ingentaconnect.com/content/10.3813/AAA.919409, doi: 10.3813/AAA.919409.

Dalmont, J.-P., Gilbert, J., and Ollivier, S. (2003). "Nonlinear characteristics of single-reed instruments: Quasistatic volume flow and reed opening measurements," *The Journal of the Acoustical Society of America* **114**(4), 2253–2262, asa.scitation.org/doi/10.1121/1.1603235, doi: 10.1121/1.1603235.

Debut, V., Kergomard, J., and Laloë, F. (2005). "Analysis and optimisation of the tuning of the twelfths for a clarinet resonator," *Applied Acoustics* **66**(4), 365–409, linkinghub.elsevier.com/retrieve/pii/S0003682X04001276, doi: 10.1016/j.apacoust.2004.08.003.

Dickens, P., Smith, J., and Wolfe, J. (2007). "Improved precision in measurements of acoustic impedance spectra using resonance-free calibration loads and controlled error distribution," *The Journal of the Acoustical Society of America* **121**(3), 1471–1481, asa.scitation.org/doi/10.1121/1.2434764, doi: 10.1121/1.2434764.

Eddy, D. (2016). "Acoustic Impedance Probe for Oboes, Bassoons, and Similar Narrow-bored Wind Instruments," in *DAGA2016 - 42nd German Annual Conference on Acoustics*, Aachen, pub.dega-akustik.de/DAGA_2016/data/articles/000484.pdf.

Ernoult, A., Chabassier, J., Rodriguez, S., and Humeau, A. (2021). "Full waveform inversion for bore reconstruction of woodwind-like instruments," *Acta Acustica* **5**, 47, acta-acustica.edpsciences.org/articles/aacus/abs/2021/01/aacus210048/aacus210048.html, doi: 10.1051/aacus/2021038 publisher: EDP Sciences.

Field, C., and Fricke, F. (1998). "Theory and applications of quarter-wave resonators: A prelude to their use for attenuating noise entering buildings through ventilation openings," *Applied Acoustics* **53**(1-3), 117–132, linkinghub.elsevier.com/retrieve/pii/S0003682X97000352, doi: 10.1016/S0003-682X(97)00035-2.

Gibiati, V., and Laloë, F. (1990). "Acoustical impedance measurements by the two-microphone-three-calibration (TMTC) method," *The Journal of the Acoustical Society of America* **88**(6), 2533–2545, asa.scitation.org/doi/10.1121/1.399975, doi: 10.1121/1.399975.

Grothe, T. (2013). "Experimental Investigation of Bassoon Acoustics," Ph.D. thesis, Technischen Universität Dresden, d-nb.info/1068447982/34.

Grothe, T. (2015). "Parameters ranges for artificial bassoon playing," in *Vienna talks*, Vienne, viennatalk2015.mdw.ac.at/proceedings/ViennaTalk2015_submission_78.pdf.

Grothe, T., and Amengual Garí, S. V. (2019). "Measurement of "Reed to Room"-Transfer Functions," *Acta Acustica united with Acustica* **105**(6), 899–903, www.ingentaconnect.com/content/10.3813/AAA.919370, doi: 10.3813/AAA.919370.

Grothe, T., and Baumgart, J. (2015). "Assessment of Bassoon Tuning Quality from Measurements under Playing Conditions," *Acta Acustica united with Acustica* **101**(2), 238–245, doi: 10.3813/AAA.918822.

Grothe, T., and Kob, M. (2019). "High resolution 3D radiation measurements on the bassoon," in *International Symposium on Music Acoustics (ISMA)*, pp. 139–145, pub.dega-akustik.de/ISMA2019/data/articles/000094.pdf.

Grothe, T., and Kob, M. (2020). "Bassoon Directivity Data" opus.hfm-detmold.de/frontdoor/index/index/docId/97.

Kergomard, J., Guillemain, P., Sanchez, P., Vergez, C., Dalmont, J.-P., Gazengel, B., and Karkar, S. (2019). "Role of the Resonator Geometry on the Pressure Spectrum of Reed Conical Instruments," *Acta Acustica united with Acustica* **105**(2), 368–380, www.ingentaconnect.com/content/10.3813/AAA.919320, doi: 10.3813/AAA.919320.

Kergomard, J., Guillemain, P., Silva, F., and Karkar, S. (2016). "Idealized digital models for conical reed instruments, with focus on the internal pressure waveform," *The Journal of the Acoustical Society of America* **139**(2), 927–937, asa.scitation.org/doi/10.1121/1.4942185, doi: 10.1121/1.4942185.

Kergomard, J., and Heinrich, J.-M. (1975). "Le basson," *Bulletin du GAM* (82-83), www.lam.jussieu.fr/index.php?page=BulletinsGAM.

Le Roux, J. C., Dalmont, J. P., and Gazengel, B. (2008). "A new impedance tube for large frequency band measurement of absorbing materials," in *Acoustics 2008*, Paris, www.conforg.fr/acoustics2008/cdrom/data/articles/003579.pdf.

Lefebvre, A., and Scavone, G. P. (2012). "Characterization of woodwind instrument toneholes with the finite element method," *The Journal of the Acoustical Society of America* **131**(4), 3153–3163, asa.scitation.org/doi/abs/10.1121/1.3685481, doi: doi:10.1121/1.3685481.

- Nederveen, C. J. (1998). *Acoustical aspects of woodwind instruments*, (orig. 1969) revised ed. (Northern Illinois University Press), repository.tudelft.nl/islandora/object/uuid:01b56232-d1c8-4394-902d-e5e51b9ec223.
- Openwind (2022). “Open Wind INstrument Design” openwind.inria.fr/.
- Petersen, E. A., Colinot, T., Silva, F., and H.-Turcotte, V. (2021). “The bassoon tonehole lattice: Links between the open and closed holes and the radiated sound spectrum,” *The Journal of the Acoustical Society of America* **150**(1), 398–409, asa.scitation.org/doi/10.1121/10.0005627, doi: [10.1121/10.0005627](https://doi.org/10.1121/10.0005627).
- Petersen, E. A., Guillemain, P., and Jousserand, M. (2022). “The dual influence of the reed resonance frequency and tonehole lattice cutoff frequency on sound production and radiation of a clarinet-like instrument,” *The Journal of the Acoustical Society of America* **151**(6), 3780–3791, asa.scitation.org/doi/10.1121/10.0011467, doi: [10.1121/10.0011467](https://doi.org/10.1121/10.0011467).
- Pierce, A. D. (1989). *Acoustics: An Introduction to Its Physical Principles and Applications*, 3rd edition (2019) ed. (Springer International Publishing), link.springer.com/10.1007/978-3-030-11214-1.
- Rabiner, L., and Schafer, R. (1978). *Digital Processing of speech signals*.
- Silva, F., Guillemain, P., Kergomard, J., Mallaroni, B., and Norris, A. N. (2009). “Approximation formulae for the acoustic radiation impedance of a cylindrical pipe,” *Journal of Sound and Vibration* **322**(1–2), 255–263, www.sciencedirect.com/science/article/pii/S0022460X08009085, doi: [10.1016/j.jsv.2008.11.008](https://doi.org/10.1016/j.jsv.2008.11.008).
- Tang, S. K. (2012). “Narrow sidebranch arrays for low frequency duct noise control,” *The Journal of the Acoustical Society of America* **132**(5), 3086–3097, asa.scitation.org/doi/10.1121/1.4756951, doi: [10.1121/1.4756951](https://doi.org/10.1121/1.4756951).
- Thibault, A., and Chabassier, J. (2020). “Time-domain simulation of a dissipative reed instrument,” in *Forum Acusticum*, Lyon, France, p. 6, hal.inria.fr/hal-03132474/.
- Thibault, A., and Chabassier, J. (2021). “Dissipative time-domain one-dimensional model for viscothermal acoustic propagation in wind instruments,” *The Journal of the Acoustical Society of America* **150**(2), 1165–1175, asa.scitation.org/doi/10.1121/10.0005537, doi: [10.1121/10.0005537](https://doi.org/10.1121/10.0005537).
- Tournemene, R., and Chabassier, J. (2019). “A comparison of a one-dimensional finite element method and the transfer matrix method for the computation of wind music instrument impedance,” *Acta Acustica united with Acustica* **5**, 838, www.ingentaconnect.com/content/dav/aaua/2019/00000105/00000005/art00014, doi: [10.3813/AAA.919364](https://doi.org/10.3813/AAA.919364).
- Zwikker, C., and Kosten, C. W. (1949). *Sound absorbing materials* (Elsevier).